JOINT EUROPEAN TORUS

JET–P(91)33

R. Giannella, N.C. Hawkes, L. Lauro Taroni, M. Mattioli,
J. O'Rourke, D. Pasini and JET Team

Comparison of Impurity and Electron Particle Transport in JET Discharges

Comparison of Impurity and Electron Particle Transport in JET Discharges

R. Giannella, N.C. Hawkes[1], L. Lauro Taroni, M. Mattioli[2], J. O'Rourke, D. Pasini and JET Team*

JET-Joint Undertaking, Culham Science Centre, OX14 3DB, Abingdon, UK

[1]UKAEA Euratom Association, Culham, UK
[2]CEA Euratom Association, Cadarache, France
** See Appendix 1*

Preprint of Paper to be submitted for publication in
Plasma Physics and Controlled Fusion

COMPARISON OF IMPURITY AND ELECTRON PARTICLE TRANSPORT IN JET DISCHARGES

R. Giannella, N.C. Hawkes[+], L. Lauro Taroni, M. Mattioli[*], J. O' Rourke, D. Pasini

JET Joint Undertaking, Abingdon, Oxon OX14 3EA, U.K.

+ UKAEA Euratom Association, Culham, U.K.
* C.E.A. Euratom Association, Cadarache, France

Abstract - A zone of reduced anomalous diffusivity for impurities in the central region of the discharge has been reported from several tokamaks. In this paper we point out that this condition is not an occasional occurrence, but a very general feature. Indeed all JET cases analyzed where the experimental conditions allow adequate sensitivity and space resolution for the measurement of the impurities diffusion coefficient show unambiguously that this quantity is close to neoclassical levels within $r = 0.4 \cdot a$. Furthermore, from the analysis of the electron density profile in sawtooth free phases of JET discharges with moderate electron temperature, we deduce that the electron particle diffusivity D_p is also close to neoclassical in the same region. The values obtained for D_p in that region during the early pre-sawtooth phases are the same as in ohmic post pellet phases.

INTRODUCTION

The transport of impurities in the bulk plasma of tokamak discharges is known to be dominated by a large anomalous diffusivity that in most cases results in a low impurity confinement (see for example MARMAR et al. 1982, ENGELHARDT 1987, STRATTON et al. 1989), although cases of impurity accumulation in the plasma centre and or long confinement times have been reported (e.g. by ISLER et al. 1985, FUSSMANN et al. 1989, GIANNELLA et al. 1989). The analysis of the time evolution of line integrated spectral intensities as monitored from a single line-of-sight does not allow good spatial resolution for the transport parameters. When the confinement time is

low, these signals are normally consistent with a uniform diffusion coefficient $D_{imp} \geq 0.5$ m^2/sec and a convection velocity V_{imp} that varies linearly with the minor radius. On the other hand steady state profiles are only sensitive to the ratio of V_{imp} to D_{imp} in the absence of sources.

Temporal and spatial resolution of transient events are needed to separate D_{imp} and V_{imp} and to analyze their profiles in the plasma core. Based on such analysis cases have been reported (COMPANT LA FONTAINE et al. 1985, IDA et al. 1987, KAUFMANN et al. 1989) where a strong reduction of D_{imp} is required in the central region to account for the experimental data. In JET these cases extend to a wide variety of conditions.

The aim of this paper is to draw together the disparate observations of reduced transport in the plasma core of the JET tokamak into a general picture and to compare the behaviour of impurities in this region with that of the background plasma particles. In the first section we discuss briefly the experimental observations available so far from different diagnostic techniques and in different plasma operation scenarios and comment on the generality of these results. In the following section we show that the electron density profiles observed during the current rise imply that the spatial structure of the particle diffusion coefficient for electrons has the same spatial structure as that for the impurities. Some results of modelling with reduced core diffusivity are also described in this section. A short conclusion section completes the paper.

REDUCED IMPURITY TRANSPORT IN THE CORE OF JET DISCHARGES

Due to its large size and the long time-scales involved the JET tokamak is better suited for spatial analysis of transport phenomena than smaller size machines, although, as discussed below, in most cases the experimental conditions are far from ideal for the analysis of transport parameters in the plasma centre. The cases where a clear reduction of the impurity diffusion was detected unambiguously on our machine extend to a variety of operative conditions and plasma parameters. These cases are briefly listed below.

a) Accumulation of intrinsic impurities - Impurities are seen to accumulate in the centre of the discharge when the electron density profile is well peaked on axis for a sufficient time. A necessary condition for this occurrence is the absence of sawtooth activity.

i) these conditions are often met after pellet injection (BEHRINGER et al. 1989). In such cases, where high deuteron density gradients are attained in the central region, large neoclassical inward velocities arise for impurities leading to their progressive accumulation in the plasma centre over a time scale of 1 to 2 seconds. The high level of peaking reached by the impurity density profiles implies that D_{imp} is lower than about 0.1 m^2/s within $r = 0.4 \cdot a$.

ii) On a longer time scale and in connection with less pronounced peaking of the density profile, impurity accumulation has also been detected in the early phases of the discharge before the sawteeth activity starts (GILL et al. 1991)

No impurity accumulation is observed during monster sawteeth. However this cannot be interpreted as evidence of high central D_{imp}. In fact, even in those cases where some peaking of the density and temperature profiles of the background plasma is observed in the plasma core during monster sawteeth, the expected neoclassical pinch on impurities remains moderate: the intrinsic impurity density profiles, therefore, only evolve on a time scale of several seconds and would not be expected to peak markedly even if the saturated steady profile were achieved during the sawtooth period.

b) Impurity injection experiments - Positive evidence of a reduced diffusivity zone in the plasma core with impurity injection experiments has been obtained in all the analyzed cases in different confinement modes and with a variety of plasma conditions:

i) In sawtoothing ohmic pulses by analysis of the injected impurity propagation between the sawtooth crashes.

ii) In ICRF heated pulses during monster sawteeth.

iii) In sawtooth free additionally heated phases. In these pulses the sawtooth activity is not suppressed or slowed down after the beginning of the additional heating (as in monster sawteeth), but is already absent before the heating starts. q(0) is larger than 1 in these cases.

Cases i) and ii) have been reported by PASINI et al. 1990. In the injection experiments listed above a fast propagation of the injected impurities from

the plasma periphery to about $r = 0.4 \cdot a$ is observed. From this radial position the propagation proceeds at much slower pace, showing a sharp transition of D_{imp} down to levels 10 to 30 times lower than outside over a distance not larger than 0.2 m.

iv) Another important case where a marked transition of D_{imp} to low levels in the plasma centre is clearly detected is that of impurity injection experiments into H-mode plasmas (PASINI et al. 1991).

c) Re-distribution of impurities after change in transport regime. This condition of particularly slow transport in the centre of the discharge and faster transport further out is also likely to appear when the transport regime at the plasma periphery is abruptly modified inducing a quick variation of the total impurity inventory in the outer region of the plasma column. A notable case where this circumstance is verified is the depletion phase following the transition back to L-mode after long lasting H-modes. In these cases, while the impurities which have built up during the H-phase are rapidly lost from most of the plasma cross section because of the sudden change in the transport regime, a typical slowly decaying narrow profile of impurity density persists in the centre of the discharge (GIANNELLA et al. 1990).

To evaluate the evidence summarized above, it is important to consider that the central zone of reduced transport in the centre and the sharp transition for D_{imp} are only likely to appear directly in the impurity density profiles in the following cases: a) during transient events where the impurity density is rapidly varying with time (e.g. impurity injection); in all such analyzed cases the zone of reduced diffusivity in the centre was clearly identified. b) when convection effects in the centre lead to pronounced shaping (e.g. accumulation) of those profiles. However impurity accumulation only occasionally occurs because in most cases the electron density profiles are not peaked and therefore the distribution of the impurities is expected to be at most very mildly peaked in the centre. Furthermore the sawtooth activity counteracts the development of any structure in that region because of its well known spreading effect on particles.

Two conclusions can be drawn about the core reduction of D_{imp}: 1) The marked spatial transition in the level of the anomalous impurity diffusion is

clearly demonstrated in JET in a variety of confinement modes, operation scenarios and plasma parameters including values of the safety factor and of its gradient in the central region, the electron density and temperature and their gradients. 2) No cases have been identified yet without the reduction of D_{imp} in the core of the discharge. It should be added that the central values of D_{imp} are generally close to neoclassical predictions. (BEHRINGER et al. 1990, PASINI et al. 1990).

REDUCED ELECTRON TRANSPORT IN THE CORE OF JET DISCHARGES

Evidence of marked reduction of the electron particle transport in the centre after pellet injection has already been reported from JET (JET TEAM 1988, BAYLOR 1990) as from other tokamaks before (e.g. GREENWALD et al. 1984, SCHMIDT et al. 1987 and KAUFMANN et al. 1988). In those cases a particularly low thermal diffusivity in that region has also been observed. The modifications induced by the pellet on the plasma conditions have been interpreted as a necessary condition for the achievement of reduced energy transport in that region. If the same assumption were made also for electron particle transport, a marked contrast would emerge with the impurities that we have shown to be affected by such an important reduction of the anomalous transport in a large variety of cases.

Difficulties in the analysis of the core electron particle transport

It is difficult to prove or disprove experimentally the existence of this zone of reduced electron transport. The considerations described above for the impurities are equally valid for the electrons. Indeed for the case of electron transport the difficulties are greater because the only neoclassical convective effect expected is the Ware pinch whose strength (measured in terms of the parameter $v \cdot r/D$) relative to the neoclassical diffusivity of electrons is much smaller than the corresponding parameter for impurities: therefore much smaller levels of peaking in the centre are expected for the electron density, if any.

The analysis with space and time resolved diagnostics of relatively fast transient phenomena, such as the evolution of the density profile after the injection of a small pellet penetrating to the boundary of the plasma (CHEETAM et al. 1987) or the propagation of the density perturbation after a sawtooth crash (HUBBARD et al. 1986; SIPS et al. 1989), has been used for the determination of the space profile of the electron particle diffusivity.

Different methods of analysis applied to such phenomena have been compared by GONDHALEKAR et al. 1989 and found to give consistent results, yielding for JET ohmic pulses (I_p = 3 MA) values for D_p of the order of 0.4 m^2/sec for values of the normalized minor radius r/a larger than $(r/a)_{min}$ = 0.3 to 0.6 and smaller than $(r/a)_{max}$ = 0.5 to 0.85. Unfortunately these techniques do not give information on the transport for $r/a \lesssim 0.3$ because of the smallness of the effects produced in that region if the original perturbation is outside (as for the shallow penetrating pellet case) or to the difficulty to diagnose the density profile with the necessary space and time resolution within the sawtooth mixing radius if the initial perturbation is produced by the sawtooth crash itself. These problems are expected to be greatly simplified and the requirements on the diagnostics much reduced if the initial perturbation is produced within the mentioned central region and if its subsequent relaxation happens on a long time scale (as in the cases of large pellets discussed below).

Even for slowly evolving or quasi-stationary cases, however, the space resolution available is not always adequate for a correct transport analysis. In particular the profiles obtained from Abel inverted interferometric data, due to the limited space resolution of the JET far infrared interferometer, often involve large distortions on the density gradients, which induce large systematic errors in the deduced transport parameters. Fig. 1 illustrates a typical effect: local features tend to be attenuated and averaged out over a wider region. Less pronounced central protuberances like those in the LIDAR profiles (SALTZMANN et al. 1988) of Fig. 2 can be strongly attenuated in the profiles from the interferometer.

Core electron transport in the pre-sawteeth ohmic phases

The profiles in Fig. 2 refer to the early phase of the discharge when the value of q(0) is larger then unity and the plasma core is still not affected by the sawtooth instability. The central peaks shown in Fig. 2 are not occasional occurrences, these profiles are typical: a systematic analysis on our data base shows that in the time interval between 1.9 and 2.1 s a high central peaking is observed in all the recorded JET LIDAR profiles related to discharges with modest edge fuelling. If we assume that the Ware pinch is causing such peaks, the particle diffusion coefficient D_{imp} must be suffering a strong reduction between r/a = 0.5 and 0.3 and its value in the centre must be about 0.02 m^2/s.

This protuberance is observed to persist for several seconds in high current discharges where the sawteeth onset is late, if they are moderately fuelled. This is exemplified by the profiles A and B of Fig. 3b. They refer to an ohmic 5 MA discharge (see fig 3a) where the average electron density was kept constant from t=5 s to t=10 s. In other discharges belonging to the same series, where the average electron density increased at a rate around $6 \cdot 10^{18} m^{-3}/s$ over the same time interval (because of higher gas puff fuelling and of moderate radio-frequency additional heating), the electron density profiles are slightly hollow and no central peaking is observed before the start of the sawtooth instability occurring at about the same time. The peak appearing in profile C, that is acquired just after the beginning of the sawtooth activity, however, is not to be interpreted as the persistence of a steady poloidally symmetric feature, because it is displaced by 10 to 15 cm towards the inner wall from the position of the magnetic axis, as identified by the peak of the soft X-ray emissivity (CHRISTIANSEN et al. 1989) and by the analysis of the magnetic measurements, and it extends across the sawteeth inversion surface. This peak, that is clearly emerging outside the statistical error bar, is the evidence of the complex particle transport phenomena related to the magnetohydrodynamic activity in the plasma centre during the sawtooth ramp; indeed it corresponds spatially with a well pronounced depression in the profile of T_e. The spatial correspondence of the peaks in profiles A and B with the peak of the soft X-ray emissivity is accurate within the error bar (~5 cm) and therefore is consistent with a simple magnetic topology and a symmetric density profile.

Modelling of the electron transport and comparison with impurities

In Fig. 4 the experimental electron density profiles at the beginning of the discharge and two seconds after the injection of a 4 mm pellet for an ohmic JET pulse are shown. It is worth noting the similarity between the two peaks. While the latter (t = 7.5 s) results from the external fuelling of the central region caused by the pellet, the former (t = 1.5 s) must have developed spontaneously and persists until a first small pellet is injected 3 s later (see Fig. 5).

Results from a simulation of a long time interval (t = 1 s to t = 9 s) during this pulse are indicated in Figs. 4 and 5. The code integrates the particle and current transport equations simultaneously. Neoclassical resistivity is used and the Ware pinch is calculated self-consistently. The

shape and values of the Ware velocity profiles (fig. 6) are not strongly sensitive to the particular shape chosen for the initial current distribution. Furthermore the pinch itself has only a minor influence on the time evolution of the post pellet profiles. The simulation was carried out using a constant particle diffusion profile for the electrons (shown in Fig. 8).

The absolute independence on time of the D_p profile required in the simulation is probably only a coincidence and would almost certainly be removed if the precision and repetition rate of the LIDAR profiles were higher than presently available. More important, it seems to us, is the finding that a sharp transition of D_p to very low values around r/a = 0.4 is already found before the injection of pellets and that this feature is very general in the early phases of the JET discharges.

After the second pellet injection in this pulse the impurities are seen to accumulate in the centre of the discharge. The analysis of the time evolution of this phenomenon shows that the anomalous impurity diffusion coefficient is much reduced in the centre (BEHRINGER et al. 1989). A satisfactory simulation is obtained assuming the same time independent transport parameters for the light (carbon) and metallic (nickel) with a D_{Imp} value at the centre about 0.1 m^2/s. The relative amounts of carbon and nickel used in the simulation were inferred from the quantitative comparison of the continuous bremsstrahlung radiation in the visible and soft X-ray spectral ranges. Experimental and simulated brightness time evolution are shown in Fig. 7a for soft X-ray and Fig. 7b for Ni XXIV and Ni XXVI line intensities. A comparison is shown in Fig. 8 between the D_p profile and the profile for D_{Imp} required in the simulation of the impurity accumulation. The lower levels of the two diffusion coefficients D_{Imp} and D_p in the centre are close to their neoclassical values for Ni and for the electrons respectively. In Fig. 9 the profile for the inward convection velocity V_{Imp} used in the simulation for carbon and nickel is shown along with the respective neoclassical values.

Analysis of the additionally heated cases

According to our previous discussion on the possibility of unambiguously identifying a zone of reduced diffusivity in the centre of the discharge, other candidate pulses for our search are a) those with monsters sawteeth and b) low density pulses with deep neutral beam fuelling. Unfortunately no

conclusive evidence could be obtained so far on these pulses because of the following reasons. a) Due to high central temperature in monsters, to the consequent low parallel electric field and low Ware pinch, only a minimal density peaking is expected and therefore no positive deduction can be made on the central particle transport based on the shape of the electron density profiles. b) For the low density beam fuelled pulses, due to the frequent sawteeth and to the low acquisition frequency of LIDAR profiles, the experimental data analyzed so far are not sufficient for an adequate study of the problem.

CONCLUSIONS

We have shown that a sharp reduction of the anomalous diffusivity of impurity ions in the plasma core is a very general feature in JET discharges: indeed no cases have been identified yet where the absence of this feature can be ascertained. We have demonstrated that the post-pellet phases, that are ideal for the detection of the same feature in the profile of the electron diffusion coefficient, are not the only cases where this can be revealed: indeed it is clearly discernible in the electron density profile in the early phases of the discharge and pre-exists the injection of pellets. The analysis of central electron transport in other plasma conditions from the presently available JET data base is made difficult by unfavourable experimental conditions. Specifically devised experiments and diagnostic arrangements seem to be required.

ACKNOWLEDGMENTS

Useful discussions and suggestions received from Drs. A. Edwards, N. Gottardi, M. Keilhacker, P. Nielsen, A. Taroni, P. Smeulders, P. Stott, P. Thomas, F. Tibone and V. Zanza are gratefully acknowledged.

REFERENCES

BAYLOR L.R. (1990) ORNL/TM-1142, Oak Ridge.

BEHRINGER K. *et al.* (1989) in *Pellet Injection and Toroidal Confinement IAEA-TECDOC*-534, Vienna, p.167.

CHEETAM *et al.* (1987) *Proc. 14th European Conf. on Controlled Fusion and Plasma Physics,* Madrid, Vol I, p. 205.

CHRISTIANSEN J.P. *et al.* (1989) *Nucl. Fus.* 29 703.

COMPANT LA FONTAINE A. *et al.* (1985) *Plasma Phys. Contr. Fus.* **27** 229.

ENGELHARDT W.W. (1987) *Phil. Trans. R. Soc. London* **A322** 79.

FUSSMANN G. *et al.* (1989) *Jour. of Nucl. Mat.* **162-164** 14.

GIANNELLA R. *et al.* (1989) *Proc. 16th European Conf. on Controlled Fusion and Plasma Physics,* Venice, Vol. I p. 209.

GIANNELLA R. *et al.* (1990) *Proc. 17th European Conf. on Controlled Fusion and Plasma Physics,* Amsterdam, Vol. I p. 247.

GILL R.D. *et al.* (1991) *Proc. 18th European Conf. on Controlled Fusion and Plasma Physics,* Berlin, Vol. II p. 49.

GONDHALEKAR *et al.* (1989) *Plasma Phys. and Contr. Nucl. Fus.* **31** 805.

GREENWALD M. *et al.* (1984) *Phys. Rev. Lett.* **53** 352.

HUBBARD *et al.* (1986) *Proc. 13th European Conf. on Controlled Fusion and Plasma Physics,* Schliersee, Vol I, p. 232.

IDA K. *et al.* (1987) *Phys. Rev. Lett.* **58** 116.

ISLER R.C. *et al.* (1985) *Phys. Rev. Lett.* **55** 2413.

JET TEAM *(Presented by G.L.Schmidt)* (1989) *Proc. 12th International Conf. on Plasma Physics and Controlled Nuclear Fusion Research,* Nice, Vol I p. 215.

KAUFMANN M. *et al.* (1988) *Nucl. Fusion* **28** 827.

KAUFMANN M. *et al.* (1989) *Proc. 12th International Conf. on Plasma Physics and Controlled Nuclear Fusion Research,* Nice, Vol 1 p. 229.

MARMAR E.S. *et al.*(1982) *Nucl. Fus.* **22** 1567.

STRATTON B.C. *et al.* (1989) *Nucl. Fus.* **29** 437.

PASINI D. *et al.* (1990) *Nucl. Fus.* **30** 2049.

PASINI D. *et al.* (1991) *Proc. 18th European Conf. on Controlled Fusion and Plasma Physics,* Berlin, Vol I p. 33, to be published in *Plasma Physics and Controlled Fusion* (1991).

SALTZMANN H. *et al.* (1988) *Rev of Scient. Instr.* **59** 1451.

SCHMIDT G.L. *et al.* (1987) *Proc. 11th International Conf. on Plasma Physics and Controlled Nuclear Fusion Research,* Kyoto, Vol 1 p 33.

SIPS A.C.C. *et al.* (1989) *Proc. 16th European Conf. on Controlled Fusion and Plasma Physics,* Venice, Vol. I p. 99.

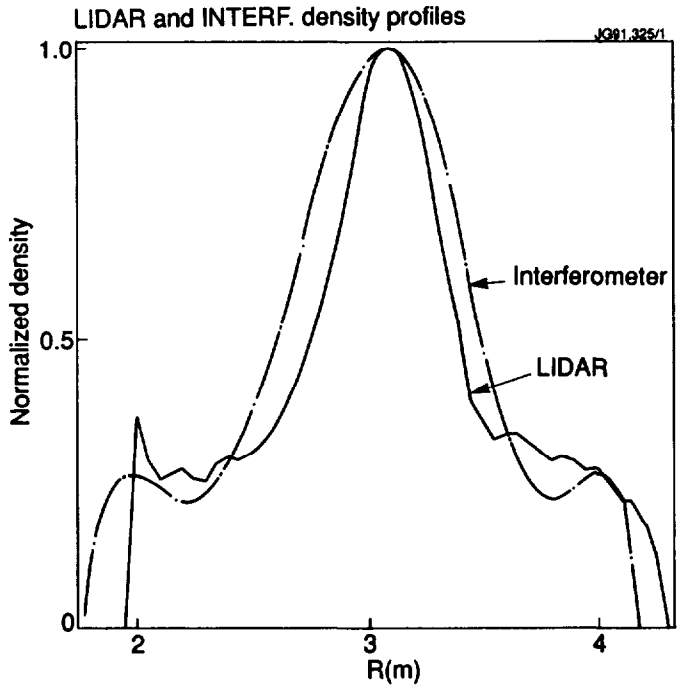

Figure 1 Comparison of the electron density profile as determined by the LIDAR diagnostics (solid line) and by Abel inversion of interferometric data (dashed line) at a time when a pronounced local feature is present. The profiles are normalized to 1 in the centre

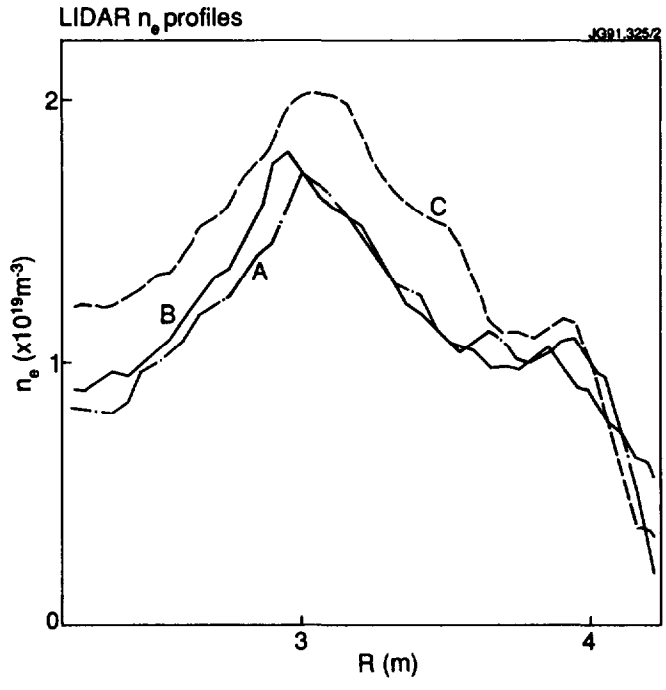

Figure 2 Typical LIDAR electron density profiles taken during the early ohmic phase of the discharge (t=2 s). JET pulse numbers are 14815 (A), 16009 (B) and 18157 (C).

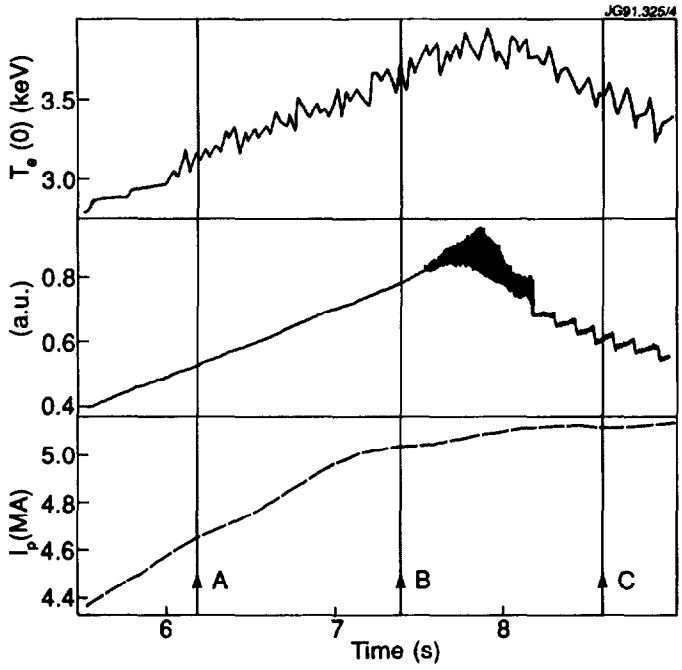

Figure 3a Peak electron temperature, soft X-ray intensity along a central horizontal line-of-sight and total plasma current for the JET pulse 23299. The timing of the three density profiles shown in figure 3b is indicated by arrows.

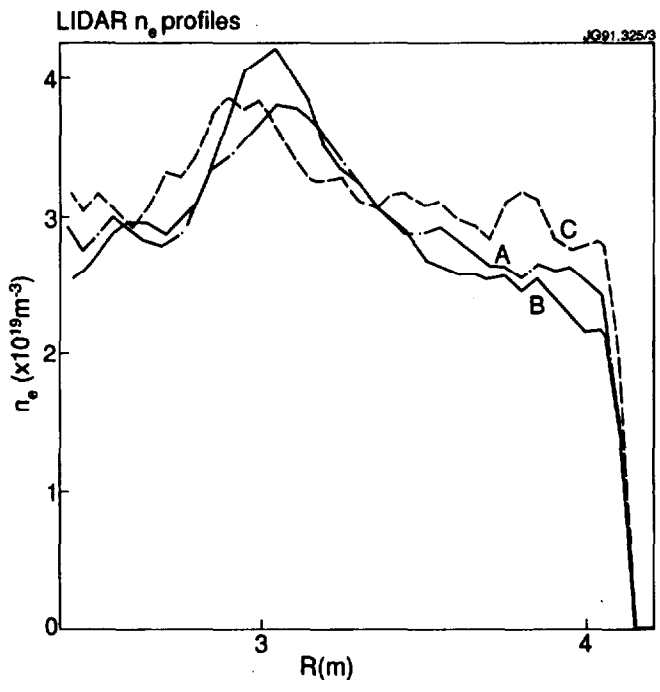

Figure 3b LIDAR electron density profiles for the pulse of Fig 3a. The central protuberance persists up to the late onset of sawtooth activity (profiles A and B). The peak in the profile acquired just after the beginning of sawteeth (C) is a poloidally asymmetric feature related to the MHD activity during the sawtooth ramp. The density level is twice as high as in fig. 2.

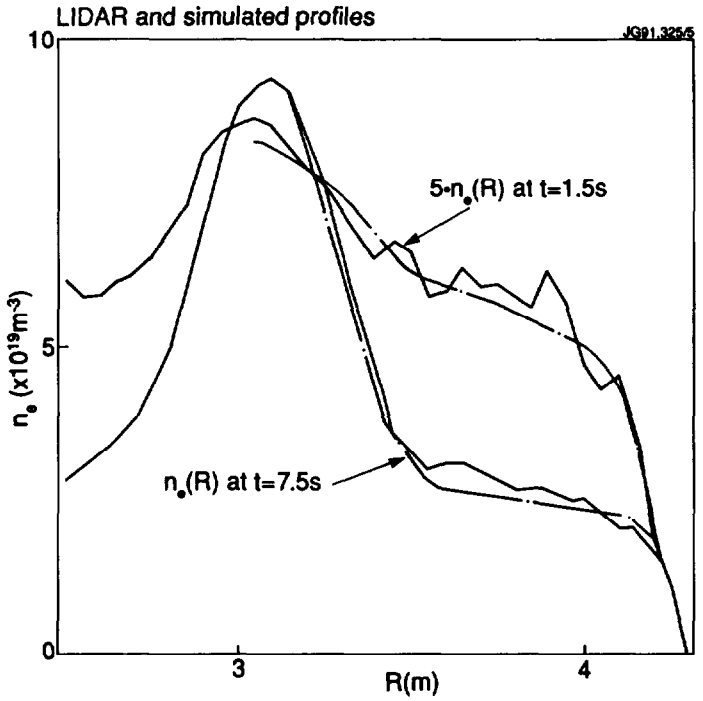

Figure 4 Experimental (solid lines) and simulated (dashed lines) electron density profiles for a JET ohmic pellet pulse (# 13572).

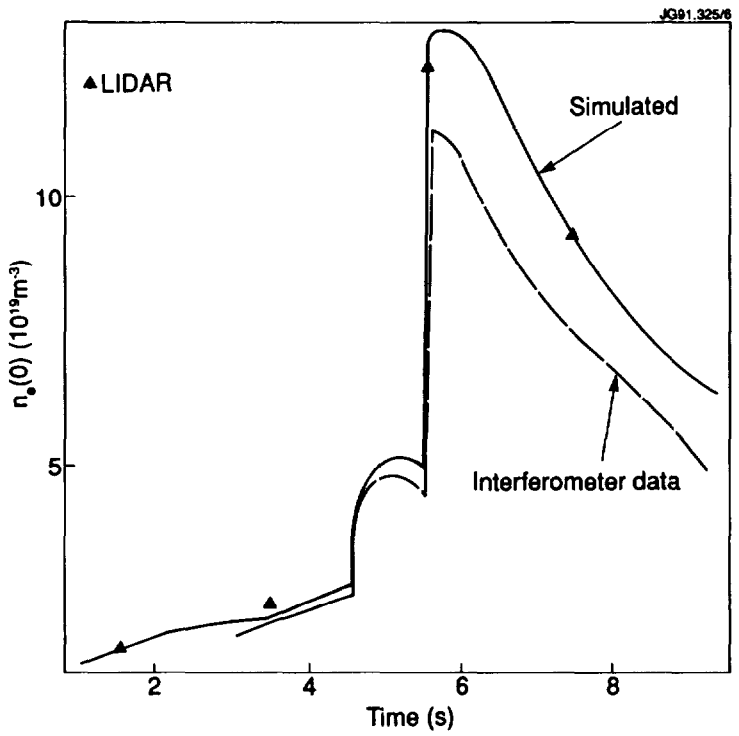

Figure 5 Time evolution of experimental (from LIDAR scattering and Abel inverted interferometric data) and simulated electron density at the centre of the discharge (JET pulse 13572).

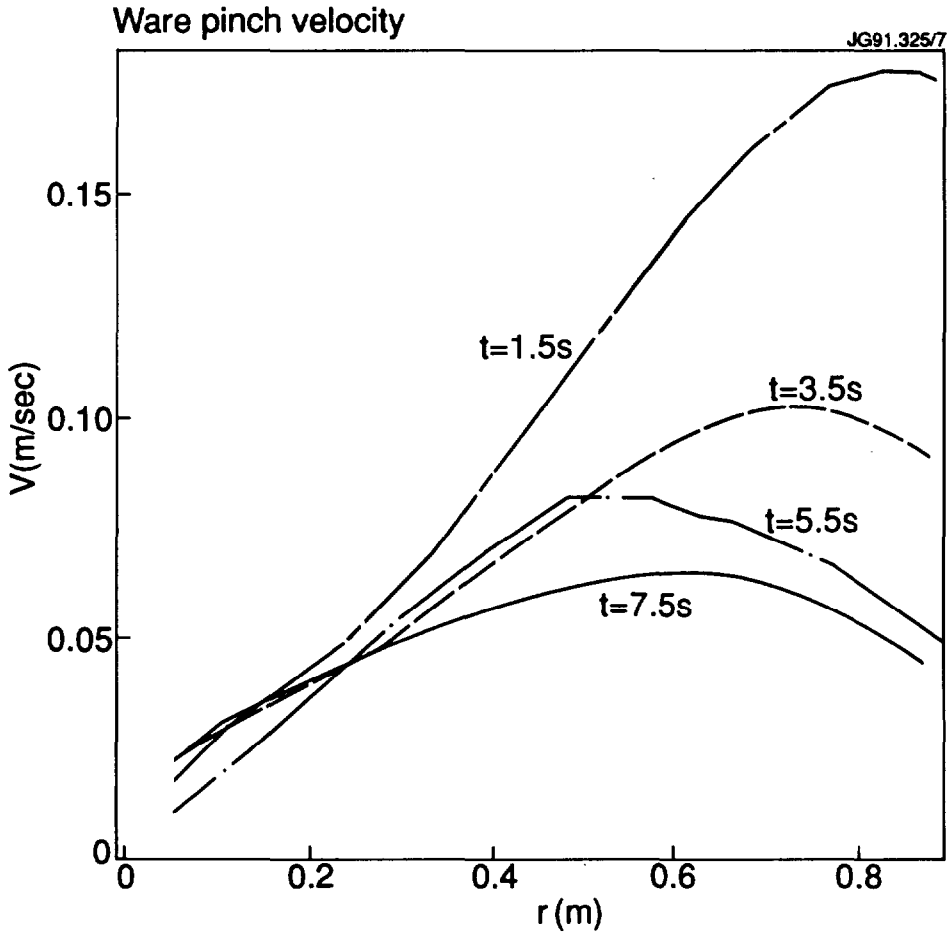

Figure 6 Radial profiles of the Ware pinch velocity at four instants during JET pulse 13572.

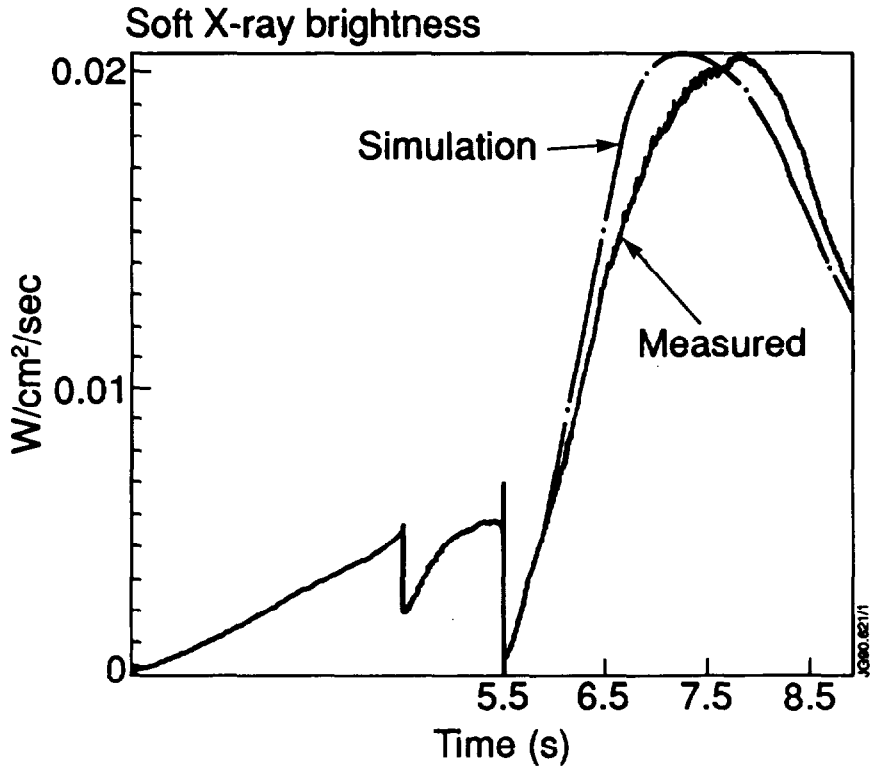

Figure 7a Experimental and simulated time evolution of soft X-ray signal measured along a central horizontal line-of-sight for JET pulse 13572.

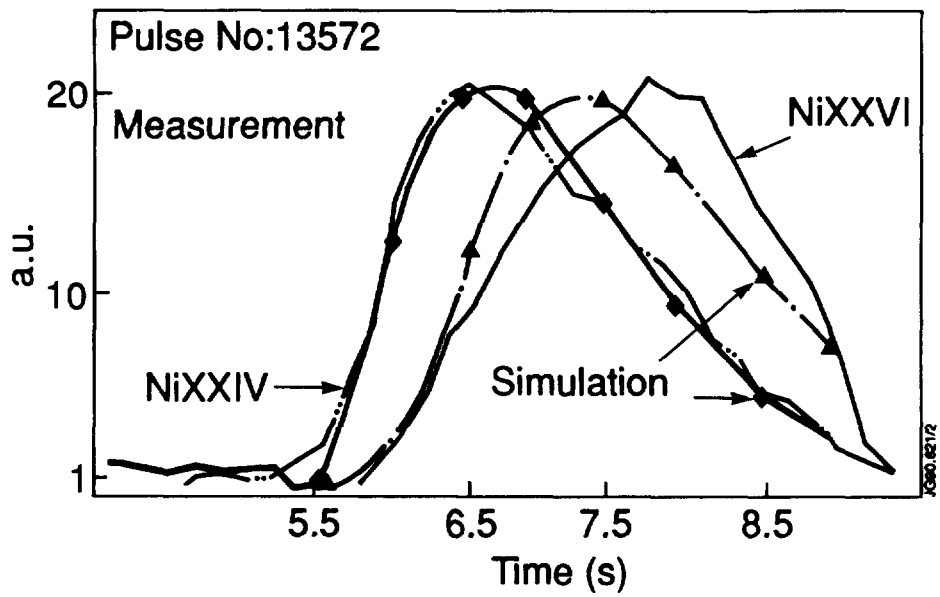

Figure 7b Experimental and simulated time evolution of the line intensities from Ni XXIV (λ=139 Å) and Ni XXVI (λ=165 Å) for JET pulse 13572.

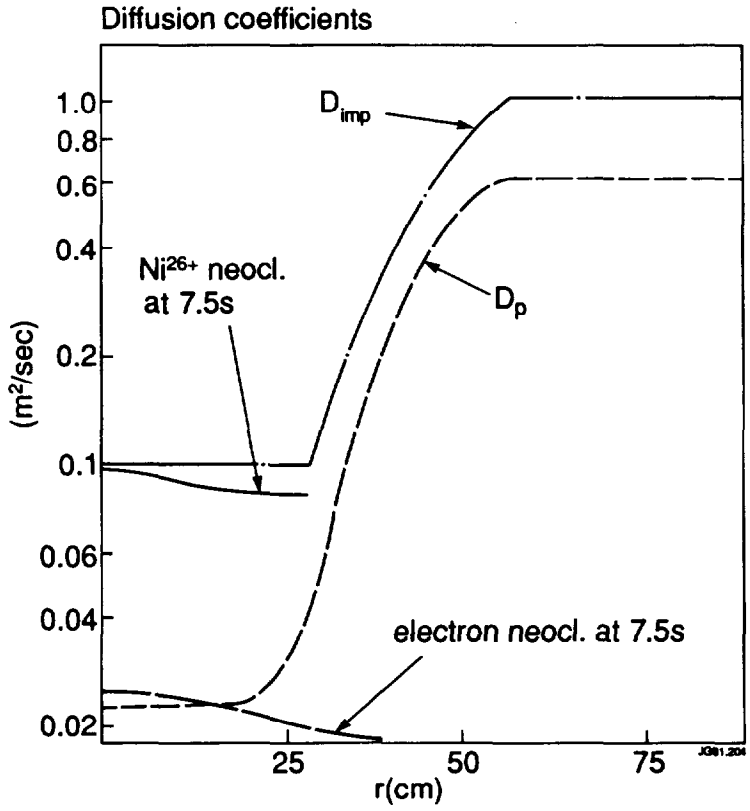

Figure 8 Radial profile of the electron and impurity diffusion coefficients for pulse 13572. Neoclassical levels at the centre are also indicated for comparison.

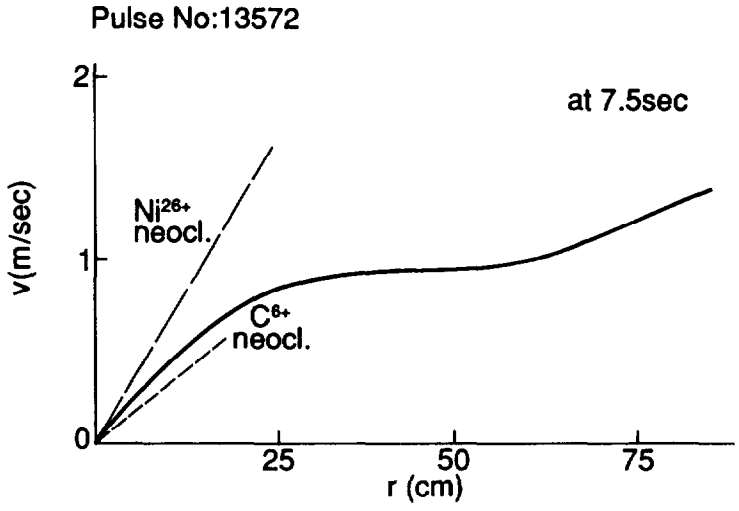

Figure 9 Radial profiles of the inward convection velocity used in the simulation of pulse 13572 for carbon and nickel. The respective neoclassical values in the centre at t=7.5 s are also shown.

Appendix I

THE JET TEAM

JET Joint Undertaking, Abingdon, Oxon, OX14 3EA, U.K.

J.M. Adams[1], H. Altmann, A. Andersen[14], P. Andrew[18], M. Angelone[29], S.A. Arshad, W. Bailey, P. Ballantyne, B. Balet, P. Barabaschi, R. Barnsley[2], M. Baronian, D.V. Bartlett, A.C. Bell, I. Benfatto[5], G. Benali, H. Bergsaker[11], P. Bertoldi, E. Bertolini, V. Bhatnagar, A.J. Bickley, H. Bindslev[14], T. Bonicelli, S.J. Booth, G. Bosia, M. Botman, D. Boucher, P. Boucquey, P. Breger, H. Brelen, H. Brinkschulte, T. Brown, M. Brusati, T. Budd, M. Bures, T. Businaro, P. Butcher, H. Buttgereit, C. Caldwell-Nichols, D.J. Campbell, P. Card, G. Celentano, C.D. Challis, A.V.Chankin[23], D. Chiron, J. Christiansen, C. Christodoulopoulos, P. Chuilon, R. Claesen, S. Clement, E. Clipsham, J.P. Coad, M. Comiskey[4], S. Conroy, M. Cooke, S. Cooper, J.G. Cordey, W. Core, G. Corrigan, S. Corti, A.E. Costley, G. Cottrell, M. Cox[7], P. Cripwell, H. de Blank[15], H. de Esch, L. de Kock, E. Deksnis, G.B. Denne-Hinnov, G. Deschamps, K.J. Dietz, S.L. Dmitrenko, J. Dobbing, N. Dolgetta, S.E. Dorling, P.G. Doyle, D.F. Düchs, H. Duquenoy, A. Edwards, J. Ehrenberg, A. Ekedahl, T. Elevant[11], S.K. Erents[7], L.G. Eriksson, H. Fajemirokun[12], H. Falter, D. Flory, J. Freiling[15], C. Froger, P. Froissard, K. Fullard, M. Gadeberg, A. Galetsas, D. Gambier, M. Garribba, P. Gaze, R. Giannella, A. Gibson, R.D. Gill, A. Girard, A. Gondhalekar, C. Gormezano, N.A. Gottardi, C. Gowers, B.J. Green, R. Haange, G Haas, A. Haigh, G. Hammett[6], C.J. Hancock, P.J. Harbour, N.C. Hawkes[7], P. Haynes[7], J.L. Hemmerich, T. Hender[7], F.B. Herzog, R.F. Herzog, J. Hoekzema, J. How, M. Huart, L Hughes, T.P. Hughes[4], M. Hugon, M. Huguet, A. Hwang[7], B. Ingram, M. Irving, J. Jacquinot, H. Jaeckel, J.F. Jaeger, G. Janeschitz[13], S. Jankowicz[22], O.N. Jarvis, F. Jensen, E.M. Jones, L.P.D.F. Jones, T.T.C. Jones, J-F. Junger, E. Junique, A. Kaye, B.E. Keen, M. Keilhacker, G.J. Kelly, W. Kerner, R. Konig, A. Konstantellos, M. Kovanen[20], G. Kramer[15], P. Kupschus, R. Lässer, J.R. Last, B. Laundy, L. Lauro-Taroni, K. Lawson[7], M. Lennholm, A. Loarte, R. Lobel, P. Lomas, M. Loughlin, C. Lowry, B. Macklin, G. Maddison[7], G. Magyar, W. Mandl[13], V. Marchese, F. Marcus, J. Mart, E. Martin, R. Martin-Solis[8], P. Massmann, G. McCracken[7], P. Meriguet, P. Miele, S.F. Mills, P. Millward, R. Mohanti[17], P.L. Mondino, A. Montvai[3], S. Moriyama[28], P. Morgan, H. Morsi, G. Murphy, M. Mynarends, R. Myrnäs[16], C. Nardone, F. Nave[21], G. Newbert, M. Newman, P. Nielsen, P. Noll, W. Obert, D. O'Brien, J. O'Rourke, R. Ostrom, M. Ottaviani, M. Pain, F. Paoletti, S. Papastergiou, D. Pasini, A. Peacock, N. Peacock[7], D. Pearson[12], R. Pepe de Silva, G. Perinic, C. Perry, M. Pick, R. Pitts[7], J. Plancoulaine, J-P. Poffé, F. Porcelli, L. Porte[19], R. Prentice, S. Puppin, S. Putvinsko[23], G. Radford[9], T. Raimondi, M.C. Ramos de Andrade, P-H. Rebut, R. Reichle, E. Righi, F. Rimini, D. Robinson[7], A. Rolfe, R.T. Ross, L. Rossi, R. Russ, P. Rutter, H.C. Sack, G. Sadler, G. Saibene, J.L. Salanave, G. Sanazzaro, A. Santagiustina, R. Sartori, C. Sborchia, P. Schild, M. Schmid, G. Schmidt[6], B. Schunke, S.M. Scott, A. Sibley, R. Simonini, A.C.C. Sips, P. Smeulders, R. Stankiewicz[27], M. Stamp, P. Stangeby[18], D.F. Start, C.A. Steed, D. Stork, P.E. Stott, T.E. Stringer, P. Stubberfield, D. Summers, H. Summers[19], L. Svensson, J.A. Tagle[21], A. Tanga, A. Taroni, A. Tesini, P.R. Thomas, E. Thompson, K. Thomsen, J.M. Todd, P. Trevalion, B. Tubbing, F. Tibone, E. Usselmann, H. van der Beken, G. Vlases, M. von Hellermann, T. Wade, C. Walker, R. Walton[6], D. Ward, M.L. Watkins, M.J. Watson, S. Weber[10], J. Wesson, T.J. Wijnands, J. Wilks, D. Wilson, T. Winkel, R. Wolf, B. Wolle[24], D. Wong, C. Woodward, Y. Wu[25], M. Wykes, I.D. Young, L. Zannelli, Y. Zhu[26], W. Zwingmann.

PERMANENT ADDRESSES

1. UKAEA, Harwell, Didcot, Oxon, UK.
2. University of Leicester, Leicester, UK.
3. Central Research Institute for Physics, Academy of Sciences, Budapest, Hungary.
4. University of Essex, Colchester, UK.
5. ENEA-CNR, Padova, Italy.
6. Princeton Plasma Physics Laboratory, New Jersey, USA.
7. UKAEA Culham Laboratory, Abingdon, Oxon, UK.
8. Universidad Complutense de Madrid, Spain.
9. Institute of Mathematics, University of Oxford, UK.
10. Freien Universität, Berlin, F.R.G.
11. Swedish Energy Research Commission, S-10072 Stockholm, Sweden.
12. Imperial College of Science and Technology, University of London, UK.
13. Max Planck Institut für Plasmaphysik, Garching bei München, FRG.
14. Risø National Laboratory, Denmark.
15. FOM Instituut voor Plasmafysica, 3430 Be Nieuwegein, The Netherlands.
16. University of Lund, Sweden.
17. North Carolina State University, Raleigh, NC, USA
18. Institute for Aerospace Studies, University of Toronto, Downsview, Ontario, Canada.
19. University of Strathclyde, 107 Rottenrow, Glasgow, UK.
20. Nuclear Engineering Laboratory, Lapeenranta University, Finland.
21. CIEMAT, Madrid, Spain.
22. Institute for Nuclear Studies, Otwock-Swierk, Poland.
23. Kurchatov Institute of Atomic Energy, Moscow, USSR
24. University of Heidelberg, Heidelberg, FRG.
25. Institute for Mechanics, Academia Sinica, Beijing, P.R. China.
26. Southwestern University of Physics, Leshan, P.R. China.
27. RCC Cyfronet, Otwock Swierk, Poland.
28. JAERI, Naka Fusion Research Establishment, Ibaraki, Japan.
29. ENEA, Frascati, Italy.

At 1st June 1991